Stabilization in relativistic photoionization with circularly polarized light

D. P. Crawford
Physics Department, The American University, Washington, D.C. 20016-8058
and W. J. Schafer Associates, Inc., 1901 North Fort Myer Drive, Arlington, Virginia 22209

H. R. Reiss
Physics Department, The American University, Washington, D.C. 20016-8058
and Institute for Theoretical Atomic and Molecular Physics, Harvard-Smithsonian Center for Astrophysics, Cambridge, Massachusetts 02138

(Received 19 August 1993; revised manuscript received 29 October 1993)

Relativistic ionization rates and related phenomena are calculated for ground-state hydrogen atoms in the presence of a circularly polarized electromagnetic field. A Dirac formalism is used, with spin effects fully included. A primary purpose of this work is to explore the effects of relativity on atomic strong-field stabilization. A wide range of frequencies is covered, and in all cases relativistic effects first dampen the stabilization phenomenon as the field intensity increases, and then strongly enhance it in the intensity domain where the ponderomotive potential exceeds the electron rest energy. Relativistic effects can produce major changes in the photoelectron energy spectrum, but perhaps the most easily observable effect is the major shift that can occur in the photoelectron angular distribution.

PACS number(s): 32.80.Rm, 32.90.+a, 42.50.Hz

I. INTRODUCTION

In previous work [1] the strong-field approximation (SFA) method was used to derive a Dirac transition-rate expression for ionization of a relativistic hydrogen atom. Results for transition rate, and for photoelectron angular distribution and spectrum, were provided for several frequencies. These results demonstrated the onset of relativistic effects by comparison with the nonrelativistic limit.

In this paper the relativistic domain has been systematically explored over a broad range of frequencies from the infrared to the far ultraviolet (or soft x ray). In doing so, we take advantage of the property of the SFA that it applies to all frequencies. We explore as well a very wide range of field intensities, in view of the increasing reliability to be expected of the method as the kinetic energy of the emitted electrons becomes increasingly dominant over the binding energy of the atomic potential. The foundation for these basic properties of the SFA is reviewed in brief in Sec. II.

Advances over the results given in [1] stem from heightened appreciation of the range of applicability of the SFA which has followed mostly from studies of stabilization [2] within the SFA and also from work on the effects of atomic state on photoionization [3,4] and of the influence of laser pulse shape in time-dependent ionization profiles [5]. In addition, improved computational algorithms and better computing facilities have made possible major extensions of the range of frequencies and intensities available for study. In this latter sense, our work takes on some of the character of "numerical experiments" as exemplified, for example, by the direct integration of the equations of motion undertaken by Kulander, Schafer, and Krause [6], or the corresponding one-dimensional calculations of Eberly *et al.* [7]. Calculations for several frequencies have been extended to the extreme relativistic domain to show how relativity affects the intensity dependence of the ionization rate in general, and the stabilization phenomenon in particular. Also shown are relativistic effects on the angular distribution and on the spectrum of the photoelectrons. Two types of results are especially dramatic. One is a sharp reduction in the total transition rate from nonrelativistic rates when the relativistic domain is fully entered. This constitutes a strong enhancement of the stabilization effect [8–10,2] in circularly polarized light. The other is a major shift toward the forward direction of the angular distribution of the photoelectrons.

It is found as well that, in the transition region between the intensity at which stabilization sets in, and that at which the problem becomes unquestionably relativistic, there is a range of intensities in which relativistic effects reduce (rather than enhance) the tendency towards stabilization. Also shown is a significant broadening of the photoelectron spectrum as a consequence of relativity.

We note that the formalism employed here is in a fully four-dimensional Dirac matrix space, so that our transition amplitude necessarily involves couplings to negative energy states. Since the theory is also nonperturbative, our final transition probabilities inherently include summation over all possible virtual electron-positron pair-production processes. The S matrix we evaluate is that for production of an ionized atom in the final state, with no physical electron pairs present. Plans for the future include treatment of the problem where electron pairs can exist in the final state.

Although the present work is stated in the simplest possible terms—monochromatic applied field, hydrogen ground state as initial state—these constraints stem simply from the fact that new ground is being explored and we wish to avoid needless complexity. The SFA method allows for the rigorous introduction of arbitrary temporal

shape of the laser pulse, and one can also introduce approximate means to represent any spatial and temporal shape of a laser pulse. With respect to initial atomic states, exact Dirac solutions are known [11,12] only for pure hydrogenic states, and they grow increasingly complicated as the quantum numbers increase. It is appropriate here to avoid adding confusing detail to an already complex calculation.

II. REVIEW OF THE THEORY

The convenience and accuracy of the SFA stem from the use of an S matrix which correctly represents laboratory boundary conditions in strong-field ionization; the utilization of this S matrix in time-reversed form, so that most of the atomic information for photoionization is placed in the initial state; the property of the time-reversed S matrix that the initial bound state of the atom is employed in a form free of the field (and hence is well known); and from the presumed dominance of the laser field in the final state. This presumption becomes more accurate the more completely this final state is dominated by the strong electromagnetic field. Unlike perturbation theory, the SFA improves as the electromagnetic field becomes stronger. The foundations of the SFA are now reviewed.

The SFA is based upon an S matrix whose exact expression is well known. It is most familiar in a nonrelativistic context, and so this will be employed first for didactic purposes. If a system is initially prepared in a state free of the transition-causing field, and the final products of the interaction are detected in a region which is also free of this field, then the "asymptotic" states are described nonrelativistically by the equation of motion

$$(i\partial_t - H_0)\Phi = 0 , \tag{1}$$

where $\partial_t \equiv \partial/\partial t$ and "natural" units with $\hbar = c = 1$ are used. In the case of an atom, H_0 contains the kinetic-energy operator as well as the atomic potential. When the external electromagnetic field is present, the equation of motion is altered to

$$(i\partial_t - H_0 - H_I)\Psi = 0 , \tag{2}$$

where

$$H_I = -e\,\mathbf{A}\cdot(-i\nabla)/m + e^2\mathbf{A}^2/2 . \tag{3}$$

The transition amplitude for the transformation from an initially noninteracting state Φ_i to a particular final noninteracting state Φ_f is given by the S matrix

$$(S-1)_{fi} = -i\int dt(\Phi_f, H_I\Psi_i) , \tag{4}$$

where Ψ_i is that solution of Eq. (2) which satisfies the asymptotic condition

$$\lim_{t\to-\infty} \Psi_i = \Phi_i . \tag{5}$$

Given a physical situation in which $\mathbf{A}$ in the H_I of Eq. (3) goes to zero outside a limited region of interaction, then Eq. (4) is *exact* as long as the wave functions Φ_f, Ψ_i are known exactly. The situation pertaining to strong-field atomic ionization is one in which the boundary conditions connected with Eq. (4) are entirely appropriate. The problem is that Ψ_i is difficult to approximate in view of the fact that, in a bound state of the atom, neither the atomic field nor the external laser field can be said to be *the* dominant influence when the laser field is very intense. For problems in strong-field ionization, it is thus useful to employ the time-reversal symmetry of the quantum-mechanical equations of motion to replace Eq. (4) with its time-reversed equivalent,

$$(S-1)_{fi} = -i\int dt(\Psi_f, H_I\Phi_i) , \tag{6}$$

where Ψ_f is that solution of Eq. (2) which satisfies the asymptotic condition

$$\lim_{t\to+\infty} \Psi_f = \Phi_f . \tag{7}$$

Equation (6) is also *exact,* with the same provisos that applied to Eq. (4). However, Ψ_f refers to an atomic state with the electron ionized. If the field is very intense, and the photoelectron emerges with kinetic energy larger than the atomic binding energy, then the influence of the laser field may be said to be dominant over that of the atomic field, and one can find a suitable simple analytical approximation for Ψ_f. Furthermore, Eq. (6) places the principal dependence on the atomic potential in the noninteracting atomic state Φ_i, which, in principle, is known with excellent accuracy. Equation (6) then provides sensitive information about the influence of atomic state on photoionization [3].

The strategy employed in the relativistic SFA is to start with the relativistic version of the time-reversed S matrix, Eq. (6),

$$(S-1)_{fi} = -i\int d^4x\,\bar{\Psi}_f e A_\mu \gamma^\mu \Phi_i , \tag{8}$$

where standard relativistic notation [11] is employed, Φ_i is now a solution of the Dirac equation

$$(i\gamma^\mu\partial_\mu - \gamma^0 V - m)\Phi = 0 \tag{9}$$

in place of the Schrödinger equation (1), Ψ_f satisfies the Dirac equation

$$(i\gamma^\mu\partial_\mu - e\gamma^\mu A_\mu - \gamma^0 V - m)\Psi = 0 \tag{10}$$

in place of the Schrödinger equation (2), V is the atomic potential, and $e\gamma^\mu A_\mu$ in Eqs. (8) and (10) plays the role of H_I in Eqs. (6) and (2).

For Eq. (8), as with Eqs. (4) and (6), the expression is an *exact* transition amplitude as long as the Φ, Ψ, and A_μ used within it are exact.

In applying Eq. (8) in the context of the SFA, we start with the fact that exact solutions are known [12,11] for the relativistic equation of motion (9) for the hydrogen atom. Thus, in the strong-field problem, we start with complete knowledge of that part (Φ_i) of Eq. (8) which contains most of the atomic information. Then two approximations are made. One (in principle not necessary) is that the laser pulse is relatively long, and so monochromatic solutions will be used for Ψ rather than the pulse-shape-dependent solutions nominally required for

Eq. (8). This is not a serious approximation as long as the laser pulse is longer than about ten wave periods [13]. Furthermore, we note that the physical boundary condition that the laser pulse goes to zero at asymptotic times is automatically enforced by the use of Eq. (8). The second approximation that is made is that the combined kinetic energy and ponderomotive energy of the emergent photoelectron is so much greater than the binding energy of the atom that one may neglect the influence of the atom on the state of the ionized electron. In support of this assertion, one may refer ahead to Figs. 6–8, showing spectra of photoelectrons at several intensities. All these figures are for a frequency (in atomic units) $\omega=\frac{1}{8}$, for ionization of ground-state hydrogen with binding energy $E_B=\frac{1}{2}$ a.u. The spectrum in Fig. 6 begins at $3.25E_B$, peaks at $4.75E_B$, and extends to about $8E_B$. For Fig. 7, the corresponding numbers are $325E_B$, $375E_B$, and $430E_B$. In Fig. 8, the comparable numbers are in the neighborhood of $38\,000E_B$. Plainly, the behavior of the photoelectron is totally dominated by the fact that it exists after ionization in the laser field. The effect of the atomic field is very small. The SFA then replaces the completely interacting state Ψ by the Volkov, or Gordon-Volkov, solution [14,15], the exact solution for a charged particle in the presence of a plane-wave electromagnetic field.

In support of the accuracy of the SFA for very intense fields, one can cite the fact that exactly correct analytical forms are obtained in the tunneling limit [13,16], and excellent agreement is obtained in comparison of the SFA with ion yield measurements [17,18,3,19] carried out at intensities sufficiently high for the SFA to be applicable. With respect to tunneling behavior, the SFA approaches exactly the dc limit [16] when the tunneling conditions $z_1 \gg 1$, $F \ll F_0$ are satisfied, where F is the amplitude of the laser electric field and F_0 is the internal atomic field. In this sense, the SFA also agrees with results obtained by Dörr, Potvliege, and Shakeshaft [20].

We remark further that several putative "tests" of the SFA [21–24] that find a lack of agreement are, in fact, all based on experiments conducted at intensities one or two orders of magnitude below the nominal requirement of $z_1 \gg 1$ for the validity of the SFA [17], where the intensity parameter z_1 is defined and discussed in Sec. III. Further experience with the SFA will undoubtedly refine the simple condition $z_1 \gg 1$. For example, results with circular polarization are less demanding than those with linear polarization, total-ion-yield experiments may be less demanding a test than spectral distributions (where the first few spectral peaks may not be accurately rendered even though the more energetic part of the spectrum is accurately treated [25]), and so on.

For future reference, we make note of the fact that there is disagreement in the literature in the way the $\mathbf{A}^2$ term is treated in the formalism for transition probability. This is the underlying reason for the fact that some treatments of atomic stabilization at high frequency and very high intensity find the process always to be dominated by single photon absorption [10,26], whereas our treatment predicts "channel closings," where the minimum number of required photons indexes upwards as the intensity increases, for high field frequencies as well as for low frequencies. We regard the formalism employed here as a strong argument for our view (other arguments are given elsewhere [27]), but the resolution of the conflict has yet to be achieved.

III. INTENSITY PARAMETERS

Three intensity parameters will be introduced here with minimal discussion. They are described in detail in Ref. [17]. The first, z_1, provides a measure of the lowest intensity for which the SFA is valid, and is defined by

$$z_1 \equiv 2U_p/E_B \ . \tag{11}$$

The ponderomotive potential of the electron in the applied electromagnetic field is U_p, and the field-free binding potential of the atom is E_B. For circularly polarized light the SFA becomes valid for $z_1 \gg 1$, which indicates the point at which the potential energy of the electron in the applied field becomes comparable to the binding energy of the atom. The second intensity parameter, z, is defined by

$$z \equiv U_p/\hbar\omega \ , \tag{12}$$

where $\hbar\omega$ is the energy of a single photon of the applied field. The condition $z < 1$ is a necessary condition for the validity of perturbation theory [13,17]. By contrast, in the numerical examples done here, $z \gg 1$ generally, and is as large as $z \approx 10^5$. The final intensity parameter, z_f, determines when relativistic effects are important. It is defined by

$$z_f \equiv 2U_p/mc^2 \ . \tag{13}$$

The denominator, mc^2, is the rest energy of the electron. When $z_f > 1$, the ponderomotive potential due to the electromagnetic field exceeds the electron rest energy, and a relativistic formulation is unquestionably required. In Eqs. (12) and (13), $\hbar$ and c, nominally equal to unity in natural units, have been restored for expository clarity.

Table I contains the six frequencies used for these calculations. Intensities at which each of the intensity parameters takes on a value of unity are provided for each frequency. In the final column are the intensities ($I_{\rm pk}$) where the peak ionization rate is predicted by the calculations. The Table indicates that this maximum ionization rate occurs in, or at the edge of, the domain of the SFA, but well below the relativistic regime (that is, $z_1 > 1$ but $z_f \ll 1$).

By exploring the intensity regime up to and beyond $z_f = 1$, the calculations provide insight into the behavior known as "stabilization." Perturbative behavior is such that the ionization rate always increases with intensity. Stabilization refers to the behavior when the ionization rate peaks and subsequently declines as the intensity increases. Our calculations provide information on the influence of relativity on stabilization.

TABLE I. Frequency-dependent intensity (in atomic units) for which the intensity parameters are unity and for which the peak (i.e., the maximum) ionization rate occurs.

Frequency	Wavelength	Intensity (a.u.) at which			I_{pk}
(a.u.)	(μm)	$z=1$	$z_1=1$	$z_f=1$	(a.u.)
$\frac{1}{128}$	5.83	2×10^{-6}	6×10^{-5}	2.3	0.087
$\frac{1}{32}$	1.46	1.2×10^{-4}	9.8×10^{-4}	37	0.091
$\frac{1}{8}$	0.365	7.8×10^{-3}	0.016	590	0.16
$\frac{1}{2}$	0.0911	0.5	0.25	9300	0.69
2	0.0228	32	4	1.5×10^{5}	17
8	0.00570	2000	64	2.4×10^{6}	1700

IV. FORMALISM

The transition amplitude stated in Eq. (8) has been applied in Ref. [1] to the calculation of a fully relativistic differential transition rate for the ionization of ground-state hydrogen. The result is

$$\frac{dW}{d\Omega}=\frac{2(eam)^2}{\pi(Z/a_0)^3}\sum_n \frac{p}{m}\frac{(u_A+u_B+u_C)}{[1+(\rho a_0/Z)^2]^4}\ , \tag{14}$$

where definitions of the key variables are given below. The quantities m and e are the mass and charge of the electron, and Ze is the nuclear charge. The parameter a is the amplitude of the vector potential of the applied field. Equation (14) follows from a Dirac treatment of the problem, including bound states, unbound states, and interaction terms. Hence, spin effects are included in full. The stated differential transition rate comes from performing an average over initial spin states of the electron, and a sum over final spins.

The momentum parameter p is

$$p=(n\omega-\eta\omega-E_B)^{1/2}(2m+n\omega-\eta\omega-E_B)^{1/2}\ , \tag{15}$$

where $\eta=(ea)^2/4p\cdot k$, ω is the field frequency, and $\rho=\mathbf{p}-(n-\eta)\mathbf{k}$.

The u quantities are

$$u_A=\tfrac{1}{4}\mathcal{P}\{[J_{n+1}(\zeta)]^2+[J_{n-1}(\zeta)]^2\}\left[\left[\frac{E}{m}-1\right]\mathcal{F}\left[\frac{\rho a_0}{Z}\right]^2+\left[\frac{E}{m}+1\right]\mathcal{G}+\frac{p}{m}\mathcal{H}\cos\theta\right]$$
$$-\mathcal{P}J_{n+1}(\zeta)J_{n-1}(\zeta)\gamma(\beta m a_0)\left[\frac{\rho a_0}{Z}\right]^2\left[\frac{p}{m}\right]^2\mathcal{U}\mathcal{V}\sin^2\theta\ , \tag{16}$$

$$u_B=-\frac{\omega n\mathcal{P}}{2m}\left[\left[\frac{\rho a_0}{Z}\right]J_n(\zeta)\right]^2\left\{\mathcal{F}-2\beta\gamma\frac{ma_0}{Z}\left[\frac{E}{m}+(n-\eta)\frac{\omega}{m}-2\frac{p}{m}\cos\theta\right]\mathcal{U}\mathcal{V}+\beta^2\mathcal{V}^2\right\}\ , \tag{17}$$

$$u_C=\frac{\omega}{m}\frac{z\mathcal{P}[J_n(\zeta)]^2}{2(E/m-p\cos\theta/m)}\left[\left[\frac{\rho a_0}{Z}\right]^2\mathcal{F}+\mathcal{G}+\mathcal{H}\right]\ , \tag{18}$$

where a_0 is the Bohr radius and

$$\beta\equiv(1-\gamma)/Z\alpha\ , \tag{19}$$

$$\gamma\equiv(1-Z^2\alpha^2)^{1/2}\ , \tag{20}$$

$$\mathcal{P}=\frac{(1+\gamma)[\Gamma(\gamma)]^2 2^{2(\gamma-1)}}{\Gamma(1+2\gamma)}\frac{[1+(\rho a_0/Z)^2]^{2-\gamma}}{(\rho a_0/Z)^6}\ , \tag{21}$$

$$\mathcal{F}=\left[\gamma\left[\frac{\rho a_0}{Z}\right]\mathcal{U}\right]^2\ , \tag{22}$$

$$\mathcal{G}=\left[\beta\left[\frac{\rho a_0}{Z}\right]\mathcal{V}\right]^2\ , \tag{23}$$

$$\mathcal{H}=2\gamma(\beta m a_0)\left[\frac{\rho a_0}{Z}\right]^2\left[\frac{p}{m}\cos\theta-(n-\eta)\frac{\omega}{m}\right]\mathcal{U}\mathcal{V}\ , \tag{24}$$

$$\chi=\gamma\arctan\left[\frac{\rho a_0}{Z}\right]\ , \tag{25}$$

$$\mathcal{U}=\sin\chi+(\rho a_0/Z)\cos\chi\ , \tag{26}$$

$$\mathcal{V}=\gamma(\rho a_0/Z)\cos\chi-[1+(1+\gamma)(\rho a_0/Z)^2]\sin\chi\ . \tag{27}$$

The θ which appears in the above is the angle between the direction of propagation of the laser field and the angle of emission of the photoelectron, while α is the fine-structure constant.

The nonrelativistic limit of this differential transition-rate expression is found in Ref. [1]. It is identical to the nonrelativistic expression derived using the SFA method and solutions to the nonrelativistic Schrödinger equation as shown in Ref. [13]:

$$\frac{dW}{d\Omega}=\frac{8\pi}{\omega}\left[\frac{E_B}{\omega}\right]^{5/2}\sum_{n=n_0}^{\infty}\frac{(n-z-E_B/\omega)^{1/2}}{(n-z)^2}[J_n(z^{1/2}\xi)]^2, \tag{28}$$

where

$$\xi=2(n-z-E_B/\omega)^{1/2}\sin\theta\ .$$

V. RESULTS AND OBSERVATIONS

The ionization rate is shown in Fig. 1, where relativistic results are represented by solid lines and nonrelativistic results by dashed lines. The curves are terminated at a lower bound of intensity determined by the point at which $z_1=1$. This is less than the nominal value of $z_1\geq 10$ for which the SFA is applicable, but it is done to improve the visibility of the maxima in the rate curves in Fig. 1, particularly in the neighborhood of $\omega=1$. Note that the maximum ionization rates occur for intensities which are well represented by the nonrelativistic limit. Relativistic effects begin to be noticeable when z_f is only about 10^{-3}, where the relativistic rate begins to become larger than the nonrelativistic, reaching about twice the nonrelativistic rate, after which it again recedes towards nonrelativistic values with a further increase in intensity. A result of special significance is that, as the field intensity increases still further, the ionization rate then declines precipitously in the extreme relativistic regime.

Figure 2 is an expanded view of the high-intensity region for four of the frequencies. The intensity at which $z_f=1$ is identified for three of the curves. Of particular interest is the rapid decline in ionization rate for $z_f>10$. According to these predictions, the atom becomes very stable for high intensities.

Reference [1] provides a simple approximation for predicting the location of the peak in the relativistic angular distribution of emitted electrons. (The nonrelativistic distribution will always be centered about 90°.) The approximation is based on consideration of the photon momen-

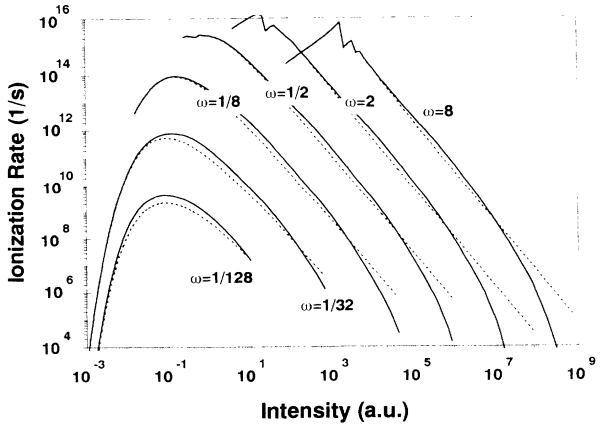

FIG. 1. Ionization rate $(1/s)$ as a function of intensity (a.u.) for six frequencies. The solid lines represent the relativistic calculation, and the dashed lines give the nonrelativistic limit.

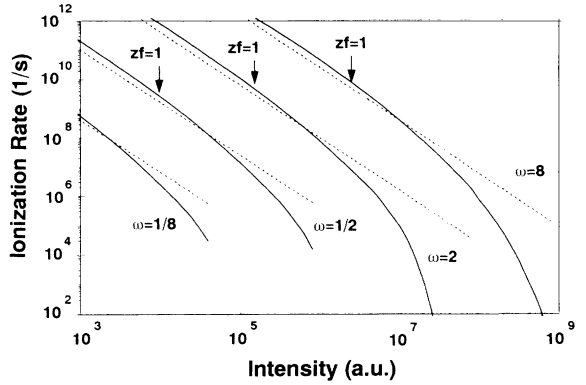

FIG. 2. Expanded view of the highest intensity part of Fig. 1, exhibiting four of the frequencies. The intensity value at which $z_f=1$ lies on this figure for three of these frequencies, and is so labeled. The solid lines represent the relativistic calculation, and the dashed lines give the nonrelativistic limit.

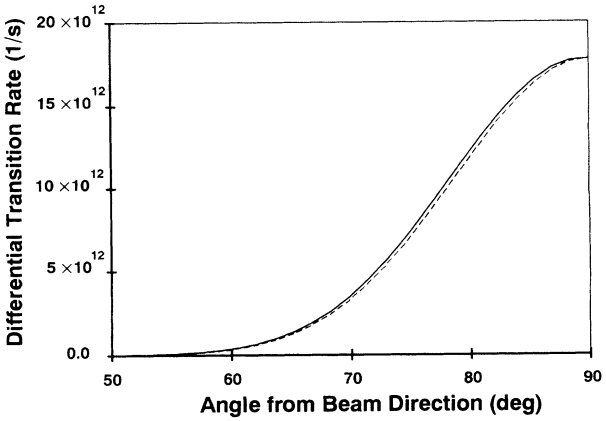

FIG. 3. The differential transition rate $(1/s)$ as a function of the angle of emission of the photoelectron as measured from the direction of propagation of the beam, for a frequency of $\frac{1}{8}$ a.u. The intensity is 0.059 a.u. corresponding to $z_f\approx 10^{-4}$. The solid line represents the relativistic calculation, and the dashed line gives the nonrelativistic limit.

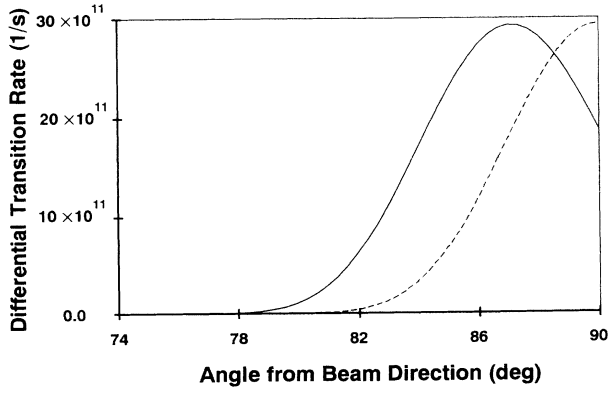

FIG. 4. The differential transition rate $(1/s)$ as a function of the angle of emission of the photoelectron as measured from the direction of propagation of the beam, for a frequency of $\frac{1}{8}$ a.u. The intensity is 5.9 a.u. corresponding to $z_f\approx 10^{-2}$. The solid line represents the relativistic calculation, and the dashed line gives the nonrelativistic limit.

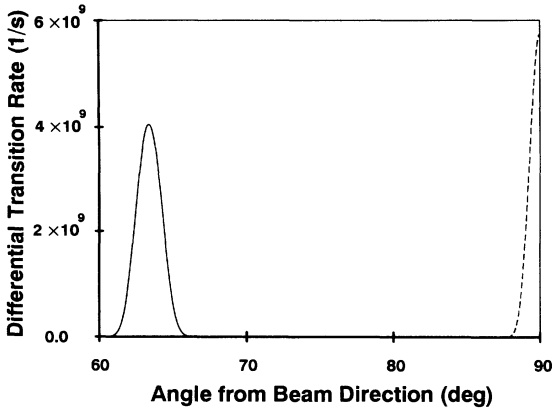

FIG. 5. The differential transition rate $(1/s)$ as a function of the angle of emission of the photoelectron as measured from the direction of propagation of the beam, for a frequency of $\frac{1}{8}$ a.u. The intensity is 590 a.u. corresponding to $z_f \approx 1$. The solid line represents the relativistic calculation, and the dashed line gives the nonrelativistic limit.

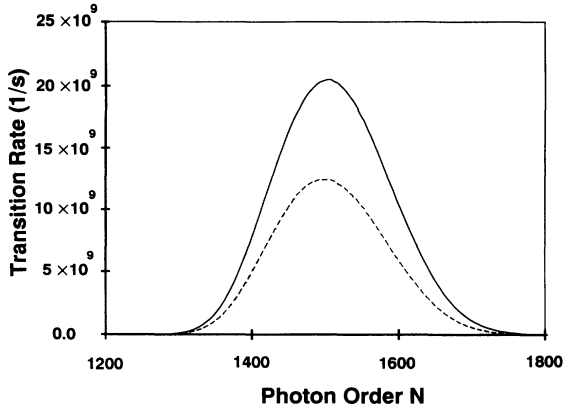

FIG. 7. The energy spectrum of the photoelectrons as given by the total transition rate as a function of the number of photons that participate in the ionization process, for a frequency of $\frac{1}{8}$ a.u. The intensity is 5.9 a.u. corresponding to $z_f \approx 10^{-2}$. The solid line represents the relativistic calculation, and the dashed line gives the nonrelativistic limit.

tum absorbed by the electron. The peak is displaced forward from the perpendicular to the beam direction by the angle

$$\theta_d \approx \arctan(z_f^{1/2}/2) \ . \tag{29}$$

Three angular distributions for a frequency of $\frac{1}{8}$ a.u. are represented in Figs. 3 through 5. Figure 3 shows the angular distribution for $z_f \approx 10^{-4}$, which is an intensity of 0.059 a.u. There is some evidence that the relativistic curve is shifted forward. The forward displacement angle, calculated using the approximation (29), is only about a quarter of a degree. In Fig. 4 the intensity is two orders of magnitude higher ($z_f \approx 10^{-2}$ and $I = 5.9$ a.u.). The relativistic distribution is clearly shifted in the direction of propagation of the incident electromagnetic field. The displacement angle approximation of Eq. (29) predicts a 2.86° forward shift, in excellent agreement with the peak shown in Fig. 4 to be near 87°. For Fig. 5 the intensity is another two orders of magnitude larger ($z_f \approx 1$ and $I = 590$ a.u.). There are two things to note. One is that the peak of the differential transition rate is much lower for the relativistic calculation. The other is that the relativistic peak, found by the detailed calculation to be near 63°, is shifted forward by the large angle of 26.6°, as predicted by Eq. (29).

If we presume the threshold of measurable angular shifts to be about 1° then the calculations predict the onset of observable relativistic effects in the angular distributions at $z_f \approx 10^{-3}$. This shows the angular distribution to be an especially sensitive measure of the appearance of relativistic effects.

Photoelectron energy spectra (as represented by the number of absorbed photons) for a frequency of $\frac{1}{8}$ a.u. are

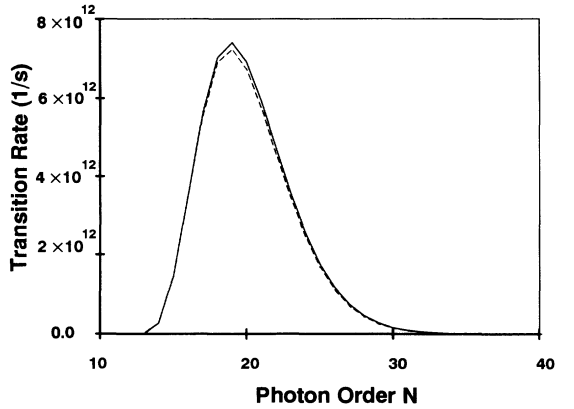

FIG. 6. The energy spectrum of the photoelectrons as given by the total transition rate as a function of the number of photons that participate in the ionization process, for a frequency of $\frac{1}{8}$ a.u. The intensity is 0.059 a.u. corresponding to $z_f \approx 10^{-4}$. The solid line represents the relativistic calculation, and the dashed line gives the nonrelativistic limit.

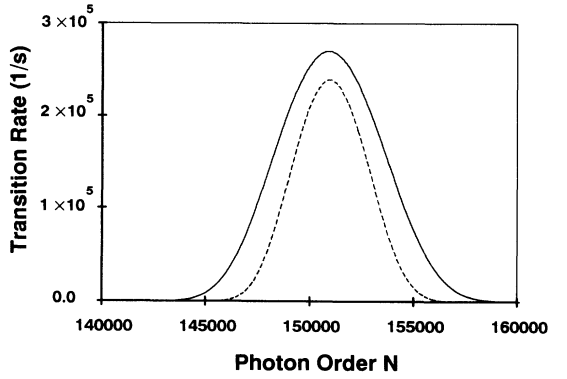

FIG. 8. The energy spectrum of the photoelectrons as given by the total transition rate as a function of the number of photons that participate in the ionization process, for a frequency of $\frac{1}{8}$ a.u. The intensity is 590 a.u. corresponding to $z_f \approx 1$. The solid line represents the relativistic calculation, and the dashed line gives the nonrelativistic limit.

given in Figs. 6 through 8 for the same three field intensities employed in Figs. 3 through 5. The spectra shown in Fig. 6 ($z_f \approx 10^{-4}$ and $I = 0.059$ a.u.) exhibit the first evidence of relativistic effects. In Fig. 7 ($z_f \approx 10^{-2}$ and $I = 5.9$ a.u.) the effects are clear. The peak of the relativistic energy spectrum is depressed as compared to the nonrelativistic spectrum. The trend is less pronounced in Fig. 8 where the intensity is one hundred times higher ($z_f \approx 1$) and $I = 590$ a.u.) because $z_f = 1$ is near the crossing point shown in Fig. 1. These predictions of the electron spectra indicate that observable consequences of relativity should become apparent around $z_f = 10^{-2}$. The threshold intensities identified above are achievable with existing lasers.

ACKNOWLEDGMENTS

This research was partially supported by the National Science Foundation under Grant No. PHY-9113926, and was also partially supported by the National Science Foundation through a grant for the Institute for Theoretical Atomic and Molecular Physics at Harvard University and the Smithsonian Astrophysical Observatory.

[1] H. R. Reiss, J. Opt. Soc. Am. B **7**, 574 (1990).
[2] H. R. Reiss, Phys. Rev. A **46**, 391 (1992).
[3] H. R. Reiss and N. Hatzilambrou, in *Super-Intense Laser-Atom Physics,* edited by B. Piraux, A. L'Huillier, and K. Rzazewski (Plenum, New York, 1993).
[4] R. S Bardfield and H. R. Reiss, Bull. Am. Phys. Soc. **35**, 1020 (1990).
[5] H. R. Reiss, N. Hatzilambrou, and D. P. Crawford, Laser Phys. **3**, 285 (1993).
[6] K. C. Kulander, K. J. Schafer, and J. L. Krause, in *Atoms in Intense Laser Fields,* edited by M. Gavrila (Academic, San Diego, 1992).
[7] J. H. Eberly, R. Grobe, C. K. Law, and Q. Su, in *Atoms in Intense Laser Fields,* Ref. [6].
[8] M. Pont, N. R. Walet, and M. Gavrila, Phys Rev. A **41**, 477 (1990).
[9] M. Pont and M. Gavrila, Phys. Rev. Lett. **65**, 2362 (1990).
[10] M. Gavrila, in *Atoms in Intense Laser Fields,* Ref. [6].
[11] J. D. Bjorken and S. D. Drell, *Relativistic Quantum Mechanics* (McGraw-Hill, New York, 1964).
[12] H. A. Bethe and E. E. Salpeter, *Quantum Mechanics of One- and Two-Electron Atoms* (Springer-Verlag, Berlin, 1957).
[13] H. R. Reiss, Phys. Rev. A **22**, 1786 (1980).
[14] D. M. Volkov, Z. Phys. **94**, 250 (1935).
[15] W. Gordon, Z. Phys. **40**, 117 (1926).
[16] M. V. Ammosov and V. P. Krainov, Laser Phys. **3**, 214 (1993).
[17] H. R. Reiss, Prog. Quantum Electron. **16**, 1 (1992).
[18] P. B. Corkum, N. H. Burnett, and F. Brunel, Phys. Rev. Lett. **62**, 1259 (1989).
[19] R. S. Bardfield and H. R. Reiss, Bull. Am. Phys. Soc. **36**, 1249 (1991).
[20] M. Dörr, R. M. Potvliege, and R. Shakeshaft, Phys. Rev. Lett. **64**, 2003 (1990).
[21] P. H. Bucksbaum, L. Van Woerkom, R. R. Freeman, and D. W. Schumacher, Phys. Rev. A **41**, 4119 (1990).
[22] M. Bashkansky, P. H. Bucksbaum, and D. W. Schumacher, Phys. Rev. Lett. **60**, 2458 (1988).
[23] R. R. Freeman and P. H. Bucksbaum, J. Phys. B **24**, 325 (1991).
[24] R. R. Freeman, P. H. Bucksbaum, W. E. Cooke, G. Gibson, T. J. McIlrath, and L. D. van Woerkom, in *Atoms in Intense Laser Fields,* Ref. [6].
[25] H. R. Reiss, in *Photons and Continuum States of Atoms and Molecules,* edited by N. K. Rahman, C. Guidotti, and M. Allegrini (Springer-Verlag, Berlin, 1987).
[26] M. Dörr, R. M. Potvliege, D. Proulx, and R. Shakeshaft, Phys. Rev. **43**, 3729 (1991).
[27] H. R. Reiss, Phys. Rev. A **42**, 1476 (1990).